PISTON LUBRICATION IN RECIPROCATING COMPRESSORS

A. T. Prata*

J. R. S. Fernandes
Department of Mechanical Engineering
Federal University of Santa Catarina
88040-900 Florianópolis, SC - BRAZIL
voice: (55) 48-234 5166 / fax: (55) 48-234 1519
e-mail: prata@nrva.ufsc.br

F. Fagotti
Brazilian Compressor Industry - EMBRACO
89219-901 Joinville, SC BRAZIL

ABSTRACT

Piston dynamics plays a fundamental role in two critical processes related to fluid flow in reciprocating compressors. The first is the refrigerant leakage through the radial clearance, which may cause considerable loss in the pumping efficiency of the compressor. The second process is the viscous friction associated with the lubricant film in the radial clearance; certainly a significant factor in the compressor energy consumption. In the present contribution a numerical simulation of the piston movement inside the cylinder of a reciprocating compressor is performed. The compressor considered here is a small hermetic compressor employed in domestic refrigerators. For the problem formulation both the axial and the radial piston motion is considered. In operation, the piston moves up and down along the axis of the cylinder, but the radial oscillatory motion in the cylinder bore, despite being usually small, plays a very important role on the compressor performance and reliability. The compromise between sealing of the gas leakage through the piston-cylinder clearance and the friction losses requires a detailed analysis of the oscillatory motion for a good design. The forces acting on the piston are the hydrodynamic force due to the pressure build up in the oil film (lubrication effects), the force due to the connecting rod, the viscous force associated with the relative motion between the piston and oil, and the force exerted by the gas on the top of the piston. All corresponding moments are also included in the problem formulation of the piston dynamics, in order to determine the piston trajectory, velocity and acceleration at each time step. The hydrodynamic force is obtained from the integration of the pressure distribution on the piston skirt, which, in turn, is determined from a finite volume solution of the time dependent equation that governs the oil flow. A Newton-Raphson procedure was employed in solving the equations of the piston dynamics. The results explored the effects of some design parameters and operating conditions on the stability of the piston, its sealing performance and friction losses. Emphasis was placed on investigating the influence of the pin location, radial clearance and oil viscosity on the piston dynamics. The complexity of the piston movement in reciprocating compressors was demonstrated and the detailed model presented can be employed as an useful tool for engineering design.

INTRODUCTION

The forces acting on a piston as it goes up and down in a reciprocating engine are the force due to the compressed gas acting on the top of the piston, the connecting rod force, the normal force due to the hydrodynamic pressure developed in the oil film between the piston and cylinder bore, the force resulting from the piston inertia and the friction force. Those forces and the corresponding moments due to the hydrodynamic and the friction forces are represented in figure 1. As a result of those unbalanced forces, in addition to the piston movement up and down small translations and rotations can occur. It has long been recognized that these oscillatory

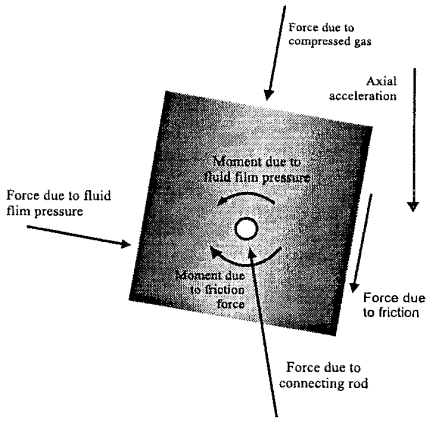

Fig. 1 - Force and moments acting on a piston

* Corresponding author

motions are very important to engine performance and reliability. Therefore, all the major concern in designing those systems, such as gas leakage, frictional power loss, noise and anti-wear life, are significantly related to the mutual dependence between the piston dynamics and the lubrication. In small reciprocating compressors employed in domestic refrigerators, extremely low friction loss is required and ringless piston are commonly used to eliminate the friction between the piston skirt and cylinder wall. In those ringless compressors the sealing of the pressure differential across the piston skirt is obtained only by the small radial clearance between piston and cylinder. A compromise then has to be achieved between a radial clearance that is small enough to prevent gas leakage and large enough to avoid significant friction loss. To fully benefit from lower friction and minimum gas leakage in ringless piston, any contact between piston and cylinder wall must be prevented. Because of the freedom of lateral motion in ringless piston compressors, a small and stable reciprocating motion of the piston should be ensured by a thin fluid film between piston and cylinder maintained at all times. Lubrication thus plays an important role in performing a complete dynamic analysis of reciprocating pistons.

Several works available in the open literature have dealt with the lubrication characteristics between piston and cylinder in reciprocating motion. For a literature review before the eighties, on both theoretical and experimental attempts to explore piston lubrication, reference is made to Li et al. (1983). Those authors themselves have shown through an analytical model that piston skirt friction can be significantly increased if the wrist-pin is located in an unfavorable position. A brief survey, focusing on those contributions relevant to the present investigation will now be presented.

A numerical study on piston slap in diesel engines was performed by Suzuki et al. (1987) who explored the effects of arbitrary skirt surfaces and pin eccentricity in the piston dynamics. Zhu et al. (1982, 1993) numerically investigated piston motion, lubrication and friction in mixed lubrication taking into account effects of surface waviness, roughness, surface profile, bulk elastic deformation and thermal distortion of both piston skirt and cylinder bore. The proposed model was applied to a four stroke automotive engine showing that good hydrodynamic lubrication can minimize the possibility and severeness of piston impact against the cylinder bore and reduce the frictional loss.

In a sequence of three papers, Gommed and Etsion (1993, 1994) and Etsion and Gommed (1995) presented a mathematical model for analyzing the dynamics of gas lubricated ringless pistons. A relatively large size helium cryocooler was investigated and it was shown that although the cylinder piston shape is commonly used for ringless piston applications, this is not the best choice for an optimum design as far as piston stability and sealing performance are concerned. Other piston shapes were explored and an improved design was obtained with noncylindrical profiles.

Theoretical and experimental results were obtained by Yamaguchi (1994) for two piston-cylinder assemblies. One operating in the standard mode, with hydrodynamic lubrication, and other operating with oil being injected in the radial clearance between piston and cylinder. It was shown for low crankshaft velocities, that the hydrostatic piston can operate with reduced friction and same oil leakage as the hydrodynamic piston as long as the radial clearance is made small.

Lee (1994) proposed a piston with tilted top for an internal combustion engine that is able to employ the combustion gas force in favor of the piston stability. The elastohydrodynamic lubrication was investigated by Dursunkaya et al. (1994) for a diesel engine. It was shown that surface deformation can play a significant role in the piston secondary motion.

None of the works previously cited dealt with piston lubrication in reciprocating compressors. In this regard the main objective of the present work is to perform, for the first time, a dynamic analysis for the thin fluid film between piston and cylinder in presence of oscillatory secondary motion occurring in small refrigerating compressors. The complete set of equations describing both piston and connecting rod motion are formulated. Those equations allow the prediction of the spatial and time varying radial clearance, required for the lubrication equation.

PROBLEM FORMULATION

A typical piston-cylinder system encountered in small reciprocating compressors is depicted in figure 2. The piston, with radius R and length L is driven in a reciprocating motion by the action of the crankshaft and connecting rod. The cycle starts at the bottom dead center where $\tau = 0°$ and ends at the same point with $\tau = 360°$ after one revolution of the crankshaft which is rotating with a constant angular speed of w. The crankshaft is located at a distance "d" from the cylinder axis.

The gas pressure p_{cyl} and p_{suc}, above and below the piston, respectively, are known. For the type of application

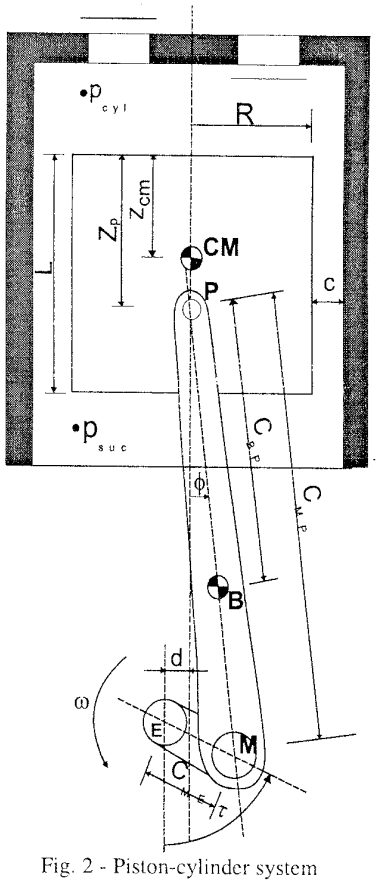

Fig. 2 - Piston-cylinder system

being considered here, p_{suc} is the compressor suction pressure and is assumed to be constant. On the top of the piston, the pressure p_{cyl} is a known function of time. A typical variation of pressure with time is presented in figure 3. Those curves can be experimentally determined, as is the case in figure 3, calculated from thermodynamic models, which is the standard procedure in compressors simulation codes (Todescat et al., 1992, Fagotti et al., 1994), or computed from energy and momentum equations (Catto and Prata, 1997).

Piston orientation within the cylinder bore are shown in figure 4. As discussed previously, unbalanced forces acting on the piston can cause rotary and translatory motions within the confinement of the cylinder clearance. Only rotation is shown in figure 4. The piston location can be described by the top and bottom skirt eccentricities, e_t, and e_b, respectively, with respect to the cylinder axis. The radial velocities of the top and bottom parts of the piston skirt are, respectively, $\dot{e}_t$ and $\dot{e}_b$; the corresponding accelerations are $\ddot{e}_t$ and $\ddot{e}_b$. It should be noted that e_t and e_b are functions of time and should be predicted by solving the piston equations of motion. The use of e_t and e_b in describing the piston location is equivalent of using the eccentricity measured from the cylinder axis to the center of mass of the piston, e_{CM}, and the tilt angle g with respect to the cylinder axis (Gommed and Etsion, 1993). The piston axial velocity and acceleration are V_p and A_p, respectively. All the motions (rotation, radial and axial translation) take place in a plane parallel to the cylinder axis and perpendicular to the wrist-pin axis.

Two coordinate systems shown in figure 5 are employed in solving the problem. System XYZ has its origin, O', fixed at the cylinder top; the Z direction coincides with the cylinder axis, and X lies on the plane of the piston motion. The system XYZ is used to formulate the equations governing the piston dynamics. Another coordinate system, rθz, has its origin, O, at the top of the piston and moves with the piston velocity V_p. The moving polar system, rθ, is parallel to the XY plane of the fixed system, XYZ, and is employed to calculate the hydrodynamic induced pressure throughout the radial clearance.

In writing the governing equations of the problem, some basic assumptions are adopted. First it is assumed that the radial clearance c, shown with exaggerated dimension in figures 2, 4 and 5, is much smaller than the piston radius. Thus, radial variation of pressure in the fluid film is negligible. Furthermore, all solid parts are rigid, and no deformation occurs. The oil flow is laminar and because the radial clearance is much smaller than the piston length, L, entrance effects are ignored. Oil is considered to be a newtonian fluid with all properties constant; a fully flooded lubrication condition is assumed.

With the aid of figures 1 and 4, and considering that all motions occur in plane XY as indicated in figure 5, the equations describing the piston dynamics can be written as,

$$s F_h + F_{rx} = m\ddot{e}_{CM} \qquad (01)$$

$$F_g + F_f + F_{rz} = mA_p \qquad (02)$$

$$M_h + M_f = I_P\ddot{\gamma} \qquad (03)$$

where F_h is the hydrodynamic force due to the pressure in the oil film, F_g is the gas force acting on the top of the piston, F_f is the viscous friction force due to the oil movement within the radial clearance, F_{rz} and F_{rx} are respectively, the axial and radial components of the connecting rod force, m is the piston mass, I_p is the piston moment of inertia about the wrist-pin location, M_h and M_f are, respectively, the moments about the wrist-pin due to F_h and F_f, and $\ddot{\gamma}$ is the piston rotary acceleration about the wrist-pin. Because γ in figure 4 is very small, F_g and F_f are considered to be aligned with the Z axis, and F_h aligned with the X axis.

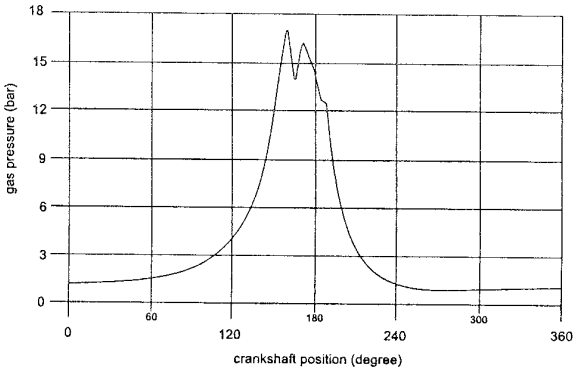

Fig. 3 - Typical instantaneous gas pressure acting on piston top

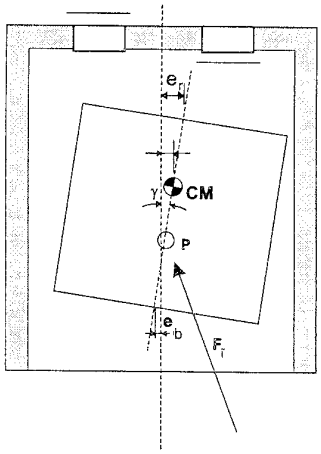

Fig. 4 - Piston orientation within the cylinder bore

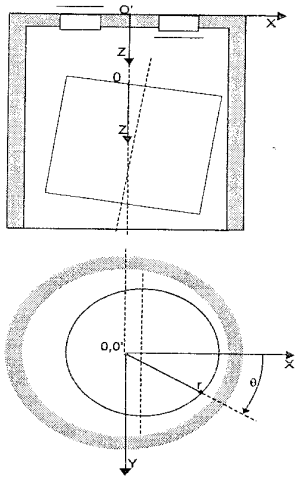

Fig. 5 - Coordinate systems employed in the solution of the problem

Due to the option of working with radial accelerations at the top and bottom of the piston, $\ddot{e}_t$ and $\ddot{e}_b$, respectively, instead of $\ddot{e}_{CM}$ and $\ddot{\gamma}$, the following equations are employed,

$$\ddot{\gamma} = (\ddot{e}_t - \ddot{e}_b)/L = c\omega^2(\ddot{\varepsilon}_t - \ddot{\varepsilon}_b)/L \quad (04)$$

$$\ddot{e}_{CM} = \ddot{e}_t - Z_{CM}\ddot{\gamma} = c\omega^2[\ddot{\varepsilon}_t - Z_{CM}(\ddot{\varepsilon}_t - \ddot{\varepsilon}_b)/L] \quad (05)$$

In writing equations (4) and (5), the time derivative was exchanged by the derivative with respect to the angle τ, where $d\tau=\omega dt$. Also, use was made of $\varepsilon_t=\varepsilon_t/c$ and $\varepsilon_b=\varepsilon_b/c$, the dimensionless eccentricities of the top and bottom of the piston, respectively.

To determine the connecting rod forces acting on the piston, F_{rx} and F_{rz}, the equations governing the connecting rod dynamics are required. To this extent, making use of the free-body diagram for the connecting rod shown in figure 6, the following equations can be written,

$$F_{Mx} - F_{rx} = m_b A_{Bx} \quad (06)$$

$$F_{Mz} - F_{rz} = m_b A_{Bz} \quad (07)$$

$$(F_{rz}C_{BP} + F_{Mz}C_{MB})\mathrm{sen}\phi - (F_{Mx}C_{MB} + F_{rx}C_{BP})\cos\phi = I_B\ddot{\phi} \quad (08)$$

In equations (6) to (8), F_{Mx} and F_{Mz} are the radial and axial components of the crankshaft force acting on the connecting rod, m_b is the connecting rod mass, A_{Bx} and A_{Bz} are, respectively, the radial and axial components of the connecting rod acceleration, C_{BP} and C_{MB} are, respectively, the distance between the connecting rod center of mass to P and to M, as indicated in figure 6; ϕ and $\ddot{\phi}$ are, respectively, the connecting rod tilting angle with respect to the cylinder axis and its angular acceleration; I_B is the connecting rod moment of inertia with respect to its center of mass, B.

The hydrodynamic force, F_h, acting on the piston skirt due to the pressure developed in the oil film, is to be obtained from the Reynolds equation. For the present situation the Reynolds equation can be written as,

$$\frac{\partial}{\partial\theta}\left(h^3\frac{\partial p}{\partial\theta}\right) + \frac{\partial}{\partial\xi}\left(h^3\frac{\partial p}{\partial\xi}\right) = -12\mu R^2\left(\frac{V_p}{2R}\frac{\partial h}{\partial\xi} - \frac{\partial h}{\partial t}\right) \quad (09)$$

where $\xi=z/R$, μ is the oil viscosity and h is the local oil film thickness. For an eccentric and tilted piston, h can be obtained from,

$$h = c\left\{1 - \left[\varepsilon_t - (\varepsilon_t - \varepsilon_b)\xi\frac{R}{L}\right]\cos\theta\right\} \quad (10)$$

Associated to equation (9), the following boundary conditions are employed,

$$\xi = 0 \ , \ p = p_{cyl} \quad \text{and} \quad \xi = L/R \ , \ p = p_{suc} \quad (11)$$

in which p_{cyl} and p_{suc} are the pressure above and below the piston, respectively, as previously discussed. Along the circumferential direction, θ, a periodic boundary condition is imposed, $p(\theta)=p(\theta+2\pi\theta)$, Symmetry along q was not employed here allowing for more generality of the computer code being developed.

Once the pressure in the oil film is known, both F_h and M_h can be determined from, respectively,

$$F_h = -\int_0^L\int_0^{2\pi} p(\theta,z)R\cos\theta d\theta dz \quad (12)$$

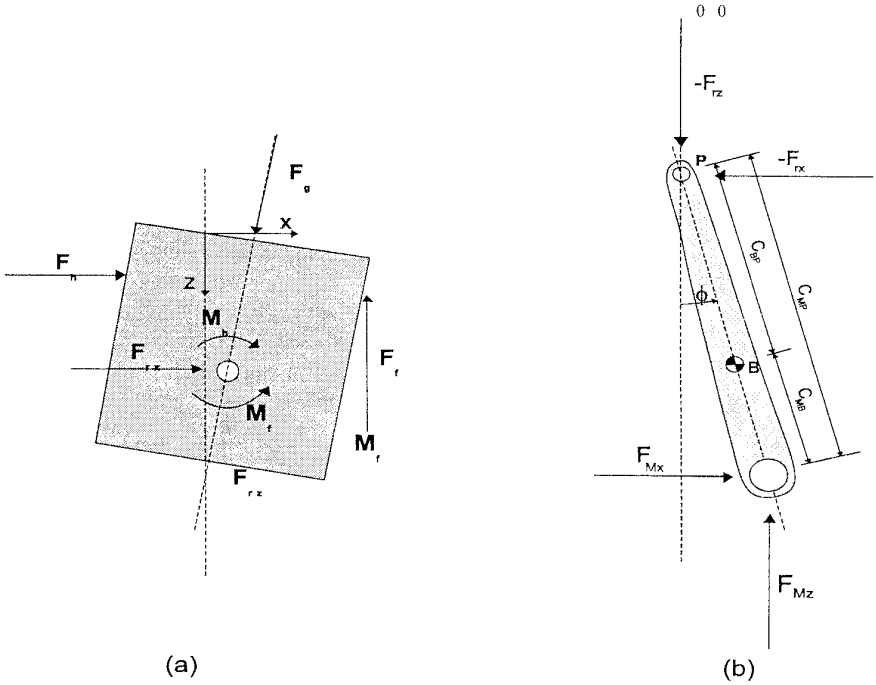

(a) (b)

Fig. 6 - Free-body diagram for: (a) piston, and (b) connecting rod

and

$$M_h = -\int_0^L \int_0^{2\pi} [p(\theta,z)R\cos\theta](z_p - z)d\theta dz \qquad (13)$$

where z_p is the wrist-pin location from the top of the piston. It should be noted that the cosθ appears in both equations (12) and (13) because piston motion is allowed only on the plane that is parallel to the cylinder axis and perpendicular to the wrist-pin axis.

From the piston motion and oil flow, the viscous frictional force and moment may be computed according to

$$F_f = -\int_0^L \int_0^{2\pi} \left(\frac{h}{2}\frac{\partial p}{\partial z} + \mu\frac{V_p}{h} \right) R d\theta dz \qquad (14)$$

and

$$M_f = -\int_0^L \int_0^{2\pi} \left(\frac{h}{2}\frac{\partial p}{\partial z} + \mu\frac{V_p}{h} \right) R\cos\theta \cdot R d\theta dz \qquad (15)$$

respectively.

The force due to the compressed gas, F_g is simply,

$$F_g = \pi R^2 (p_{cyl} - p_{suc}) \qquad (16)$$

At this moment, the problem formulation has been completed. The kinematics of crankshaft-connecting rod system yields expressions for determining the piston velocity and acceleration, V_P and A_P, respectively, as well as the components A_{BX} and A_{BZ} of the connecting rod acceleration, and the connecting rod tilting angle, ϕ, together with its acceleration, $\ddot{\phi}$. All those quantities are to be expressed in terms of the crankshaft angle, τ.

MATHEMATICAL MODEL

The equations for the piston and connecting rod dynamics, equations (1)-(3) and (6)-(8), respectively, can be combined into only two differential equations. To that extent, F_{rz} from equation (2) is first substituted into equation (7), resulting in an equation for F_{Mz} in terms of F_g and F_f. Next, F_{Mx} from equation (6) is substituted into equation (8) yielding, after substitution for the previous equation for F_{rz} and F_{Mz}, the following equation,

$$F_{rx} = [(mA_P - F_g - F_f)C_{BP} + (m_b A_{Bz} + mA_P - F_g - F_f)C_{MB}) + - C_{MB} m_b A_{Bx} - I_B\ddot{\phi}/\cos\phi]/(C_{MB} + C_{BP}) \qquad (17)$$

Now, substituting equations (4) and (5) into equations (1) and (3), respectively, results in,

$$F_h + F_{rx} = mc\omega^2[\ddot{\varepsilon}_t - z_{CM}(\ddot{\varepsilon}_t - \ddot{\varepsilon}_b)/L] \qquad (18)$$

$$M_h + M_f = I_p c\omega^2(\ddot{\varepsilon}_t - \ddot{\varepsilon}_b)/L \qquad (19)$$

The piston trajectory in terms of e_t and e_b as a function of the crankshaft angle t can now be calculated from equations (18) and (19). Required in those equations are F_h, F_{rx}, M_h and M_f, which can be obtained, respectively, from equations (12), (17), (13) and (15).

NUMERICAL METHODOLOGY

The numerical solution of equations (18) and (19) starts with prescribed values for e_t, e_b, $\dot{e}_t$ and $\dot{e}_b$. Because the piston trajectory inside the cylinder is periodic, the converged solution should not depend on the initial guess. For simplicity it is assumed that, at τ=0, $e_t = e_b = \dot{e}_t = \dot{e}_b = 0$.

An implicit formulation is employed here and from the initial values the crankshaft angle is advanced and from the geometrical parameters and the equations for the kinematics of the crankshaft-connecting rod system, values of piston velocity and acceleration along Z and connecting rod acceleration are determined for τ+Δt. From figure 3, p_{cyl} for t+Δt is also obtained. An iterative process is then needed to determine the piston radial position and velocity at time τ+Δτ, that is $\varepsilon_t^{\tau+\Delta\tau}$, $\varepsilon_b^{\tau+\Delta\tau}$, $\dot{\varepsilon}_t^{\tau+\Delta\tau}$, $\dot{\varepsilon}_b^{\tau+\Delta\tau}$. This is performed using a Newton-Raphson procedure to search for the $\dot{\varepsilon}_t^{\tau+\Delta\tau}$ and $\dot{\varepsilon}_b^{\tau+\Delta\tau}$ values that would satisfy equations (18) and (19). Values of both piston radial position and acceleration are obtained from the radial velocities $\dot{\varepsilon}_t^{\tau}$ and $\dot{\varepsilon}_b^{\tau}$ as,

$$\varepsilon_t^{\tau+\Delta\tau} = \varepsilon_t^{\tau} + \dot{\varepsilon}_t^{\tau+\Delta\tau}\cdot\Delta\tau\ ,\ \varepsilon_b^{\tau+\Delta\tau} = \varepsilon_b^{\tau} + \dot{\varepsilon}_b^{\tau+\Delta\tau}\cdot\Delta\tau \qquad (20)$$

$$\ddot{\varepsilon}_t^{\tau+\Delta\tau} = (\dot{\varepsilon}_t^{\tau+\Delta\tau} - \dot{\varepsilon}_t^{\tau})/\Delta\tau\ ,\ \ddot{\varepsilon}_b^{\tau+\Delta\tau} = (\dot{\varepsilon}_b^{\tau+\Delta\tau} - \dot{\varepsilon}_b^{\tau})/\Delta\tau \qquad (21)$$

The pressure field required in both equations (14) and (15) to calculate F_f and M_f, respectively, is determined integrating equation (9) through a finite volume approach (Prata and Ferreira, 1990). In some situations, nonrealistic pressure values may be obtained from equation (9). Because the oil film cannot sustain pressure values smaller than the gas pressure at the edges of the piston skirt, cavitation occurs. In turn, the continuity of the oil film is lost and striae are observed in the oil flow pattern. In the present work, whenever cavitation occurred, the oil pressure were replaced by a gas pressure which value was interpolated between p_{cyl} and p_{suc}, depending on the cavitation axial location.

For the numerical solution, a typical time step corresponding to five degrees of the crankshaft angle was employed. Convergence of the Newton-Raphson algorithm at each time step was achieved at most in ten iterations. A converged periodic solution for the piston trajectory required about 300 cycles. Several tests were performed to validate the numerical code. Worth mentioning is that the work delivered to the compressed gas obtained from the area of the pv diagram constructed using the gas pressure from figure 3 when added to the energy required

to overcome friction, obtained from the viscous frictional force given by equation (14) and the instantaneous piston velocity, agreed within 0,016% with the work delivered to the connecting rod from the crankshaft and obtained through kinematics considerations.

RESULTS AND DISCUSSIONS

The results to be presented were obtained for a typical reciprocating compressor employed in domestic refrigerators. Some input data including geometric parameters of the compressor is listed in table 1.

The first results to be presented focus on the influence of some design parameters on the piston trajectory within the cylinder. Variation of the minimum dimensionless distance between piston and cylinder, $h^*_{min} = h_{min}/c$, with respect to the dimensionless wrist-pin location, $z^*_p = z_p / R$, is presented in figure 7. At $z^*_p = 1$, the wrist-pin is located at the midpoint between top and bottom of the piston. From the figure it is seen that at this location h^*_{min} has its maximum value indicating the condition of highest stability. Results for the influence of force and moment on the piston throughout a cycle indicated that in the axial direction the force due to the compressed gas, F_g, is counterbalanced by the force due to the connecting rod, with a small role played by the piston inertia and virtually no effect of the viscous friction, F_f. Along the radial direction, the force due to the connecting rod, F_{rx}, is counterbalanced by the hydrodynamic force, F_h, with no role played by the piston inertia. Similarly, the acting moments are those due to the oil film pressure, M_h, and the viscous force M_f. The tendency observed in figure 7 is in close relation to the behavior of the acting moments: the highest value of h^*_{min} occurred at $Z^*_p = 1$ where the moments have their smallest values.

Table 1 - Geometric, dynamic and operational baseline parameters used in the simulation

L^* (L/R)	2
z_P^* (z_P/R)	1.151
z_{CM}^* (z_{CM}/R)	1.053
C_{BP}^* (C_{BP}/R)	2.431
C_{MP}^* (C_{MP}/R)	3.473
C_{ME}^* (C_{ME}/R)	0.6857
d* (d/R)	0.1905
ω (rd/s)	368.6
p_{suc} (bar)	1.325
I_P^* [$I_P/(mR^2)$]	0.6038
I_B^* [$I_B/(m_b C_{MP}^2)$]	0.1896

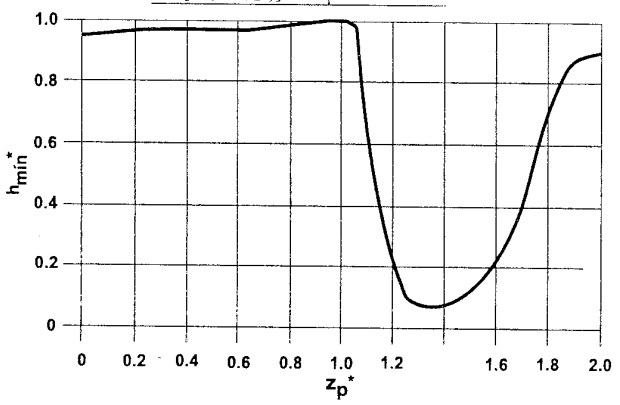

Fig.7 - Minimum local oil film thickness during a cycle as a function of wrist-pin location

To decide about the optimum wrist-pin location the results of figure 7 have to be analyzed in conjunction with results for oil leakage and power consumption. In addition to oil consumption information, oil leakage between piston skirt and cylinder bore is very important in assessing refrigerant leakage, which occurs because of the gas solubility in the oil. Gas dissolved in the oil plays an important role in reducing the compressor volumetric efficiency.

The instantaneous volumetric oil leakage throughout the clearance between piston and cylinder is given by,

$$V_\tau = \int_0^{2\pi} \left(\frac{-h^3}{12\mu R} \frac{\partial p}{\partial \xi} + V_P \frac{h}{2} \right) R d\theta \qquad (21)$$

From that, cycle average leakage can be obtained from,

$$V = \frac{1}{2\pi} \int_0^{2\pi} V_\tau d\tau \qquad (22)$$

Similarly, a cycle averaged power consumption can be calculated from,

$$P = \frac{1}{2\pi} \int_0^{2\pi} P_\tau d\tau \quad , \quad P\tau = F_f V_P \qquad (23)$$

where P_τ is the instantaneous power consumption obtained from the friction force F_f and piston velocity V_P.

Results for dimensionless power consumption, P/P_{ref}, and dimensionless volumetric oil leakage, V/V_{ref}, are shown in figure 8. From figure 7 and 8 it is seen that optimum wrist-pin location lies between $z^*_p = 0.8$ and 1.0. At this range of z^*_p, the piston operates in a stable trajectory, with low leakage and low frictional power loss. This is in close agreement to what was obtained by Gommed and Etsion (1993, 1994).

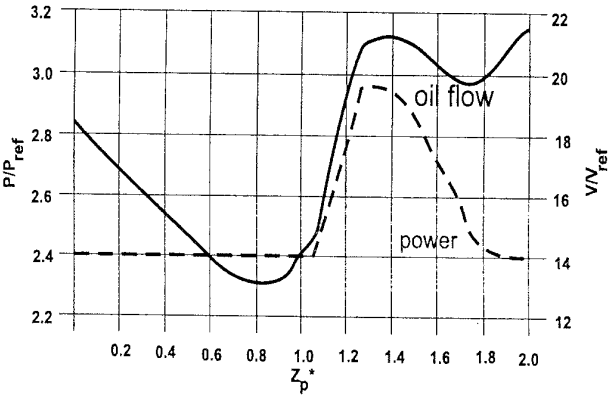

Fig. 8 - Averaged power comsumption and averaged oil leakage as a function of wrist-pin location

The increase in oil leakage for values of z^*_p greater than one, as seen in figure 8, coincides with the more unstable pattern for the piston motion observed in figure 7 for the same z^*_p values. This is so because the increase in oil leakage due to increasing values of the radial clearance at some location more than compensates for the decrease in oil leakage due to the resulting decrease in the radial clearance at the opposite locations as the piston oscillates.

The influence of the radial clearance between piston skirt and cylinder bore on the maximum value of the dimensionless eccentricity of the top and bottom during a cycle is presented in figure 9. As seen from the figure, the piston becomes more unstable as the radial clearance is increased, which was also observed by Li et al. (1983), Zhu et al. (1992) and Gommed and Etsion (1994). Smaller values of clearance c result in increasing damping of the oil films which, in turn, tend to stabilize the piston.

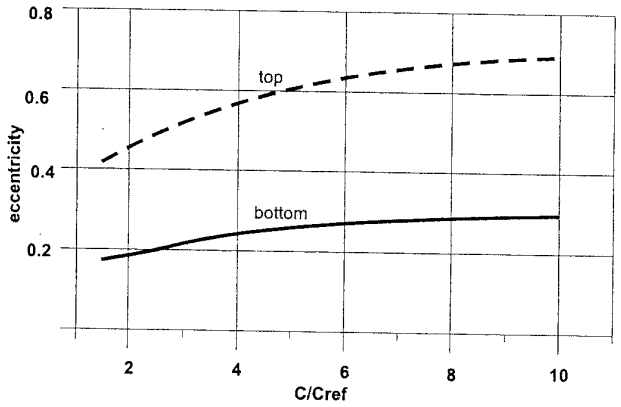

Fig. 9 - Maximum eccentricity of top and bottom during a cycle as a function of skirt-tobore radial clearance

From the stability point of view, the smaller the radial clearance the better the design. However, as shown in figure 10, small values of c results in considerable demand for power to overcome viscous friction. From figure 10, it is seen that a compromise can be achieved between power consumption and oil leakage, which is around $c/c_{ref}=6$. At this value figure 9 yields maximum eccentricities of 0.63 and 0.27 for top and bottom of piston skirt, respectively.

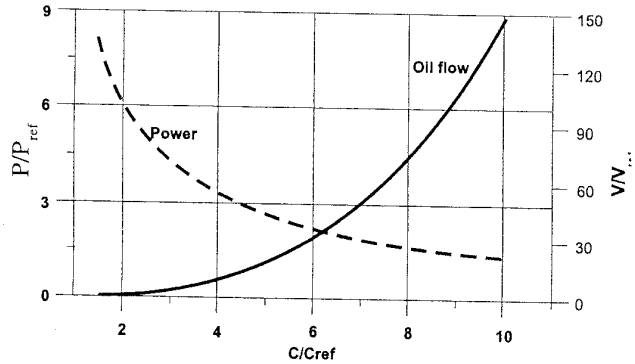

Fig. 10 - Averaged power comsumption and averaged oil leakage as a function of skirt-to-bore radial clearance

The effect of lubricant viscosity on the minimum dimensionless distance between piston and cylinder, h^*_{min}, is presented in figure 11. As would be expected, the stability of the piston trajectory increases as the viscosity increases. Despite the benefit of higher stability as oil viscosity is increased, viscous friction should also be considered. As seen in figure 12, the averaged power consumption per cycle increases almost linearly with the oil viscosity. Also shown in figure 12 is the averaged oil leakage as a function of the lubricant viscosity. From the figure it is observed that viscosity plays a very important role on oil leakage for a small range of μ/μ_{ref} values. As μ/μ_{ref} is increased, the oil leakage tend to be less and less affected by viscosity.

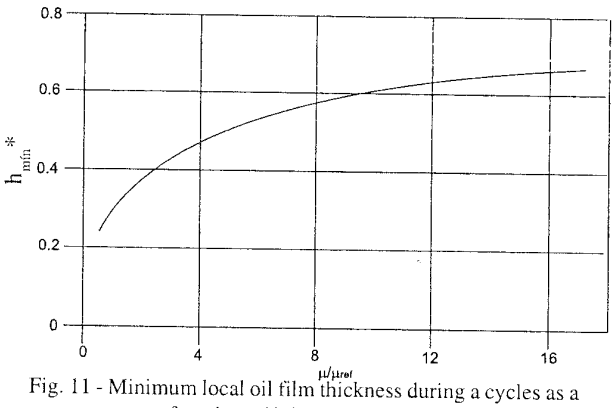

Fig. 11 - Minimum local oil film thickness during a cycles as a function of lubricant viscosity

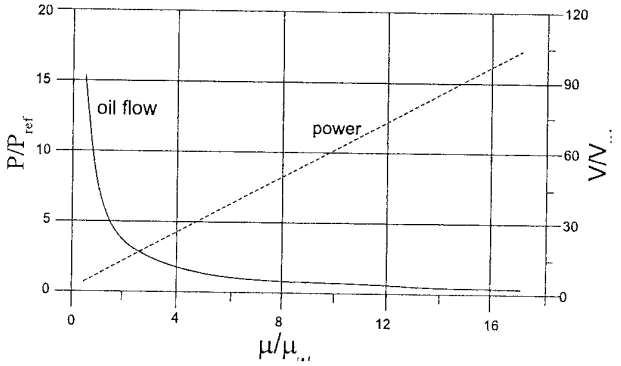

Fig. 12 - Averaged power consumption and averaged oil leakage as a function of lubricant viscosity

CONCLUSIONS

A dynamic model for piston lubrication for small reciprocating compressors was presented. Oscillatory secondary piston motion due to the unbalanced forces acting on the piston plays an important role on compressor performance and was shown to significantly affect both power consumption and oil leakage between piston skirt and cylinder bore.

The analysis incorporated equations for both piston and connecting rod dynamics as well as the lubrication equation applied to the variable shape oil film present within the confinement of the skirt-to-bore radial clearance.

Results for piston trajectory, power consumption and oil leakage were explored as a function of wrist-pin location, radial clearance between piston and cylinder, and lubricant viscosity. Among the results it was shown that undesirable piston oscillation can be significantly increased if the wrist-pin is placed below the middle of the skirt. At this location the power consumption and oil leakage presented their highest values.

There are many parameters and factors that affect piston performance which were not explored here. The model presented can be used as helpful tool in assessing the influence of length, mass, shape and location of center of mass of the piston, just to mention a few parameters. Others studies can also be

performed to investigated whether a lateral writ pin offset can be beneficial in decreasing the moments acting on the piston which would improve piston stability. Further improvements in the present model should incorporate piston and cylinder deformation, as well as skirt and cylinder contact and friction.

GREEK SYMBOLS

ε	dimensionless eccentricity
ϕ	angle between connecting rod and cylinder axis
γ	piston tilt angle
μ	viscosity of lubricant oil
θ	angular coordinate
τ	crankshaft angle
ω	crankshaft angular velocity ($\omega=d\tau/d\tau$)
ξ	dimmensionless distance along z ($\xi = z / R$)

NOMENCLATURE

A_{BX}	connecting rod acceleration along X
A_{BZ}	connecting rod acceleration along Z
A_p	piston axial acceleration
c	radial clearance between pistonand cylinder
C_{BP}	distance between wrist-pin and connecting rod center of mas
C_{MB}	connecting rod length
d	distance between connecting rod axis and culinder axis
e_{CM}	eccentricity of piston center of mass
e_t	piston top eccentricity
e_b	piston bottom eccentricity
F_f	viscous friction force
F_g	gas force
F_h	hydrodynamic force
F_M	crankshaft force
F_r	connecting rod force
h	local oil film thickness
h_{min}	minimum distance between piston and cylinder during a cycle
I_B	connecting rod moment of inertia about its center of mass
I_p	piston moment of inertia about wrist-pin
L	piston length
m	pisnton mass
m_b	connecting rod mass
M_f	viscous moment about wrist-pin
M_h	hydrodynamic moment about wrist-pin
p	oil film pressure
P	cycle averaged power consumption by viscous friction
P_τ	instantaneous power consumption by viscous friction
r	radial coordinate
R	piston radius
V_p	piston velocity
z	axial coordinate
Z_p	wrist-pin location from the top of the piston

REFERENCES

Catto, A. G. and Prata, A. T., 1997, "A Numerical Study of Instantaneous Heat Transfer During Compression and Expansion in Piston-Cylinder Geometry", *Proceedings of the ASME Advanced Energy System Division*, AES-Vol. 37, pp. 441-450, *ASME International Mechanical Engineering Congress and Exposition*, Dallas, USA.

Dursunkaya, Z., Keribar, R. and Ganapathy, V., 1994, "A Model of Piston Secondary Motion and Elastohydrodynamic Skirt Lubrication", *Journal of Tribology*, Vol. 116, pp. 777-785.

Fagotti, F., Todescat, M. L., Ferreira, R. T. S., Prata, A. T., 1994, "Heat Transfer Modeling in a Reciprocating Compressor", *Proceedings of the International Compressor Engineering Conference at Purdue*, pp. 605-610, West Lafayette, USA.

Gommed, K. and Etsion, I., 1993, "Dynamic Analysis of Gas Lubricated Reciprocating Ringless Pistons – Basic Modeling", *Journal of Tribology*, Vol. 115, pp. 207-213.

Gommed, K. and Etsion, I., 1994, "Parametric Study of the Dynamic Performance of Gas Lubricated Ringless Pistons", *Journal of Tribology*, Vol. 116, pp. 63-69.

Lee, H., 1994, "High Performance Internal Combustion Engine With Gas-Cushioned Piston", *JSME International Journal*, Series B, Vol. 37, No2. 2, pp. 434-442.

Li, D. F., Rohde, S. M. and Ezzat, H. A., 1983, "An Automotive Piston Lubrication Model", *ASLE Transactions*, Vol. 26, No. 2, pp. 151-160.

Prata, A. T. and Ferreira, R. T. S., 1990, "The Accuracy of Short Bearing Theory in Presence of Cavitation", *Journal of Tribology*, Vol. 112, pp. 650-654.

Tamaguchi, A., 1994, "Motion of the Piston in Piston Pumps and Motors", *JSME International Journal*, Series B, Vol. 37, No. 1, pp. 83-88.

Todescat, M. L., Fagotti, F., Prata, A. T. and Ferreira, R. T. S., 1992, "Thermal Energy Analysis in Reciprocating Hermetic Compressors", *Proceedings of the International Compressor Engineering Conference at Purdue*, Vol. IV, pp. 1419-1428, West Lafayette, USA.

Zhu, D., Cheng, H. S., Takayuki, A. and Hamai, K., 1992, "A Numerical Analysis for Piston Skirts in Mixed Lubrication – Part I: Basic Modeling", *Journal of Tribology*, Vol. 114, pp. 553-562.

Zhu, D., Hu, Y., Cheng, H. S., Takayuki, A. and Hamai, K., 1993, "A Numerical Analysis for Piston Skirts in Mixed Lubrication – Part II: Deformation Considerations", *Journal of Tribology*, Vol. 115, pp. 125-133.